ACS APPLIED MATERIALS & INTERFACES

Letter

www.acsami.org

Simultaneous Detection of Circulating OncomiRs from Body Fluids for Prostate Cancer Staging Using Nanographene Oxide

Mustafa Salih Hizir,[†] Mustafa Balcioglu,[†] Muhit Rana,[†] Neil M. Robertson,[†] and Mehmet V. Yigit*[,†,‡]

[†]Department of Chemistry and [‡]RNA Institute, University at Albany, SUNY, 1400 Washington Avenue, Albany, New York 12222, United States

Supporting Information

ABSTRACT: Circulating oncomiRs are highly stable diagnostic, prognostic, and therapeutic tumor biomarkers, which can reflect the status of the disease and response to cancer therapy. *miR*-141 is an oncomiR, which is overexpressed in advanced prostate cancer patients, whereas its expression is at the normal levels in the early stages of the disease. On the other hand, *miR*-21 is significantly elevated in the early stage, but not in the advanced prostate cancer. Here, we have demonstrated simultaneous detection of exogenous *miR*-21 and *miR*-141 from human body fluids including blood, urine and saliva using nanographene oxide. Our system enables us to specifically and reliably detect each oncomiR at different fluorescence emission channels from a large population of RNAs extracted from body fluids. We were also able to determine the content and the ratio of the *miR*-21 and *miR*-141 in 10 different miRNA cocktails composed of various, but unknown, concentrations of both oncomiRs. A strong agreement (around 90%) between the experimental results and the actual miRNA compositions was observed. Moreover, we have demonstrated that overexpressed *miR*-21 or *miR*-141 increases the fluorescence only at their signature wavelengths of 520 and 670 nm, respectively. The approach in this study combines two emerging fields of nanographene in biomedicine and the role of circulating miRNAs in cancer. Our strategy has the potential to address the current challenges in diagnosis, prognosis and staging of prostate cancer with a non- or minimally invasive approach.

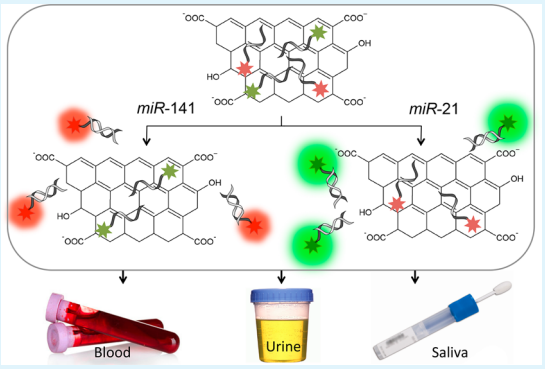

KEYWORDS: *graphene oxide, fluorescence, biosensor, body fluid, oncomiR, prostate cancer, miR-21, miR-141*

MicroRNAs (miRNAs) are small noncoding RNA molecules that regulate gene expression at the post-transcriptional level by repressing or degrading mRNAs. They are involved in the regulation of many biological processes including the cell cycle, differentiation, development and metabolism.[1] However, the role of miRNAs in human diseases such as diabetes, neurodegenerative disorders, and cancer also has been clearly demonstrated.[2,3] The expression of several miRNAs is dysregulated in cancer by a variety of mechanisms.[4] These miRNAs are referred to as oncomiRs. Studies have shown that oncomiRs are involved in the initiation, progression and metastasis of cancer, which makes them potential clinical targets for the diagnosis, prognosis, and treatment of cancer.[5,6]

OncomiRs have been isolated from tumor tissues and most of the body fluids including blood, urine, saliva, tears, semen and breast milk and are highly stable in the circulation system.[7,8] Many studies have demonstrated that circulating miRNAs remain stable after being subjected to severe settings that would normally degrade RNAs,[8,9] such as boiling, low or high pH levels, extended storage, and freeze−thaw cycles, which makes circulating oncomiRs highly stable attractive diagnostic tumor biomarkers. It has been shown that tumor cells release miRNAs into circulation and the expression levels of miRNAs in the body fluids of patients with cancer are altered significantly.[8] Moreover, circulating oncomiRs have the potential to reflect the status of the cancer.[10] For instance, the expression of a number of miRNAs in the serum of healthy men and patients with prostate cancer differed remarkably. *miR*-141 has been found highly elevated in the advanced prostate cancer patients and correlated with the serum prostate-specific antigen (PSA) level, while *miR*-21 was at normal expression levels.[8,9] On the other hand, *miR*-21 was significantly elevated in the early stage prostate cancer; however, the expression of *miR*-141 was at normal levels.[8,9,11,12] The level of miR-141 was found to be ∼46-fold overexpressed in the serum of prostate cancer patients when compared to healthy individuals. The amount of miR-141 was determined as ∼550 copies per microliter of serum of healthy individuals; however, this number was found to be ∼15650 in the serum of prostate cancer patients.[9] These results indicate that *miR*-21 and *miR*-141 are not only diagnostic tumor biomarkers but also signatures for identifying the disease stages of prostate cancer.[8]

Prostate cancer is the most common male cancer observed in the Western Hemisphere and early diagnosis of prostate cancer

Received: June 27, 2014
Accepted: August 26, 2014
Published: August 26, 2014

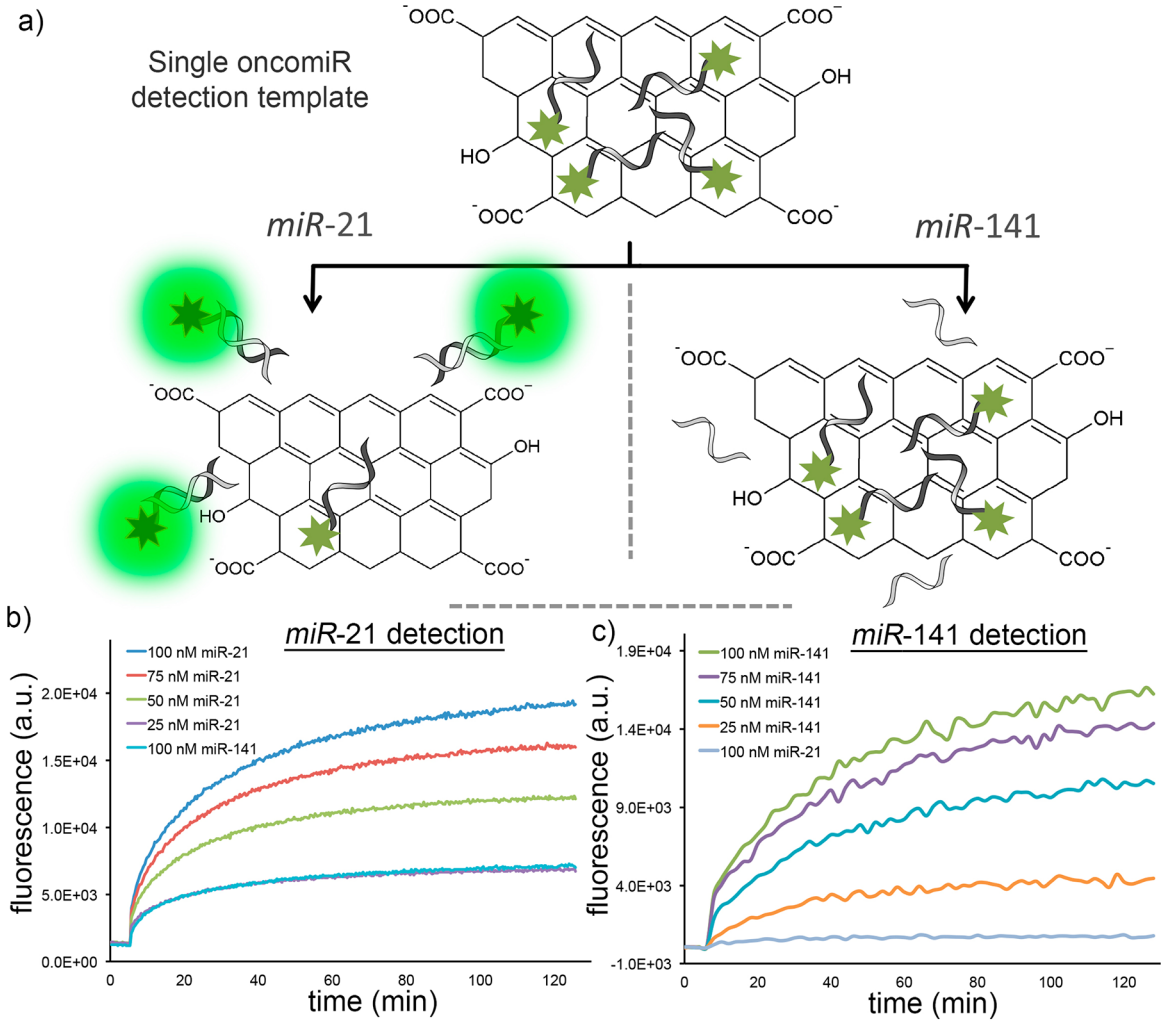

Figure 1. Engineering an assembly of nanographene and antisense probe strands for the detection of a single oncomiR. (a) Schematic representation of the nGO/FAM-anti-miR-21 assembly. The surface adsorbed probe strands hybridize to the complementary target oncomiR resulting in recovery of the fluorescence, whereas the nontarget oncomiR does not change the fluorescence because of an absence of hybridization. Fluorescence recoveries with *miR*-21 and *miR*-141 at (b) 520 nm using nGO/FAM-anti-miR-21 and (c) 670 nm using nGO/Cy5-anti-miR-141. Experiments were performed in triplicate.

is important for the survival of the patient. The current golden standard diagnosis method for prostate cancer is the detection of PSA in serum. However, the PSA testing suffers from low specificity and sensitivity. There is very high false-positive and false-negative rate associated with PSA testing.[13] These pitfalls of PSA testing raised a need for an investigation into alternative tumor biomarkers and detection approaches. Therefore, simultaneous detection of multiple oncomiRs from body fluids can enable us to identify prostate cancer and its disease stage with a non- or minimally invasive way. Here, we are demonstrating the detection of exogenous *miR*-21 and *miR*-141 individually and simultaneously from various human biological fluids using a nanotechnology platform.

Nanotechnology has influenced our life remarkably in the last two decades.[14−17] Recently, 2D nanosheets have gained significant attention due to their exciting physical properties at the two-dimensional surfaces.[18] For instance, nanographene oxide (nGO), which is a one-atom-thick, highly dispersed and stable carbon material in aqueous media, has been used for numerous advanced applications due to its extraordinary electronic, mechanical and thermal properties.[19,20] It has been used in biomedicine for the detection of disease biomarkers, delivery of genes and drugs, photothermal therapy and construction of multimodal imaging agents.[21−23] nGO has an extraordinary adsorption capacity for single stranded (ss)DNA and a fast and ultraefficient fluorescence quenching capability.[24,25] Moreover, in the presence of complementary oligonucleotides, surface-adsorbed fluorophore-labeled nucleic acids can be desorbed from the nGO surface because of hybridization, which results in the recovery of the fluorescence. Such a behavior has fascinating implications for the detection of nucleic acid binding molecules and has been utilized for proteins, nucleic acids, metal ions or small metabolites.[22,26−29] Here, we have used nanographene oxide for the simultaneous detection of circulating oncomiRs from body fluids, which are involved in the early or advanced disease stages of prostate cancer.

First, we investigated the single oncomiR detection by taking advantage of the quenching and adsorbing capability of nGO with the fluorescently labeled short oligonucleotides. Initially, FAM-labeled anti-miR-21 was assembled on the two-dimensional surface of nGO, which resulted in a fluorescently silent nGO/anti-miR-21 complex at 520 nm, (Figure 1a). Then various concentrations of *miR*-21 (25 nM, 50 nM, 75 nM, 100

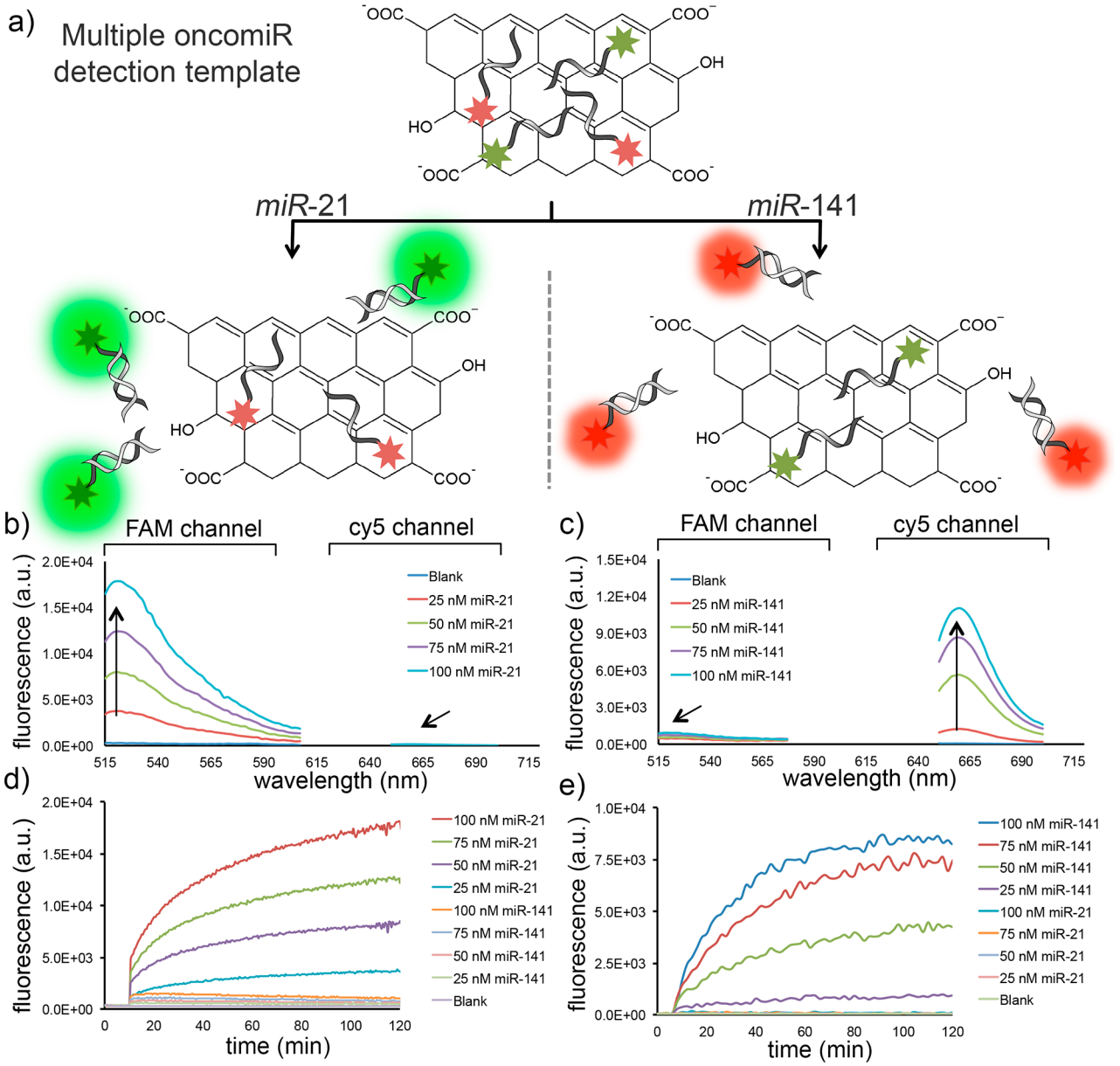

Figure 2. Engineering an assembly of nanographene and antisense probe strands for detection of two oncomiRs. (a) Schematic representation of the nGO/FAM-anti-miR-21/Cy5-anti-miR-141 assembly. The surface adsorbed probe strands hybridize to the complementary target oncomiR resulting in recovery of the fluorescence, whereas the nontarget oncomiR does not change the fluorescence due to an absence of hybridization. Fluorescence emission spectra with increasing concentrations of (b) *miR*-21 and (c) *miR*-141. Fluorescence recoveries with *miR*-21 and *miR*-141 at (d) 520 nm and (e) 670 nm. Experiments were performed in triplicate.

nM) were tested with the nGO/anti-miR-21 complex. Fluorescence intensity was collected for 2 h to observe the signal recovery due to recognition of *miR*-21 by the probe strand on nGO surface. To demonstrate the specificity of the nGO/anti-miR-21 toward the target sequence, *miR*-141 was used as a control oncomiR. Results indicate that remarkably enhanced recovery in the fluorescence signal was observed with increasing concentrations of target oncomiR (Figure 1b), whereas significantly lesser off-target effect was observed due to nonspecific replacement of the probes stands by 100 nM *miR*-141 (Figure 1b). Afterward, we performed an analogous study for detection of the *miR*-141 instead of *miR*-21. First, Cy5-labeled anti-miR-141 was adsorbed on nGO, and a similarly rapid quenching in fluorescence signal was observed at 670 nm. The fluorescently silent nGO/anti-miR-141 complex was tested with 25 nM, 50 nM, 75 nM, 100 nM *miR*-141 to demonstrate the specificity and sensitivity of the detection method. At the end of the 2-h kinetic study, higher fluorescence recoveries were observed with increasing target oncomiR (*miR*-141) concentrations (Figure 1c). However, 100 nM of the control strand (*miR*-21) resulted in almost no increase in fluorescence intensity at 670 nm (Figure 1c). The results overall suggested that each nGO/probe assembly is highly specific to the target oncomiR.

Next, we investigated a more complicated system, which enables us to detect two oncomiRs simultaneously with one nGO assembly. In order to achieve this, both FAM-labeled anti-miR-21 and Cy5-labeled anti-miR-141 were adsorbed onto the surface of same nGO template (Figure 2a). Such an assembly resulted in a fluorescently silent nGO/anti-miR-21/anti-miR-

dx.doi.org/10.1021/am504190a | ACS Appl. Mater. Interfaces 2014, 6, 14772−14778

141 complex at 520 and 670 nm. To detect different amounts of target oncomiRs selectively, we added 25, 50, 75 and 100 nM of *miR*-21 or *miR*-141 to the nGO complex (Figure 2a). Results showed that *miR*-21 resulted in an increase in the fluorescence intensity at 520 nm, however it had no effect on the fluorescence at 670 nm (Figure 2b). Whereas, *miR*-141 resulted no significant effect on the emission at 520 nm but increased the emission at 670 nm with increasing concentrations. As a result, the 520 nm (FAM channel) and 670 nm (Cy5 channel) emissions were assigned as signatures of *miR*-21 and *miR*-141, respectively. Later, 2 h kinetic studies were performed to demonstrate the fluorescence recovery over time with increasing concentrations of target and nontarget oncomiRs. As seen in Figure 2d, e, the nGO template is highly specific to both oncomiRs at different emission channels. Interestingly, this approach showed less signal-to-background ratio when compared to the single oncomiR detection method. Such a minimized off-target effect could enable us to detect the target oncomiRs more specifically. The experiments were performed for a broad range of miRNA concentrations to demonstrate the specificity, sensitivity and detection window of our design, Figure S1. The detection limit was determined as 2.0 and 1.2 nM for *miR*-21 and *miR*-141, respectively. As seen in Figure S1 in the Supporting Information, the fluorescence intensities increase with increasing concentrations of target miRNAs, and saturate around 150 nM of target miRNA because of the desorption mechanism of probe strands from the nGO surface.[30]

After validating that our second-generation template can be used to detect both oncomiRs, we explored simultaneous detection of *miR*-21 and *miR*-141. To demonstrate that, we have prepared 10 different miRNA cocktails that were composed of various, but unknown, concentrations of both oncomiRs. First, emissions at 520 and 670 nm were collected with various concentrations of *miR*-21 and *miR*-141, (Figure 3a, b). Later, these emission values were used to compare the results obtained with the unknown samples. Afterward, each unknown oncomiR cocktail was added to a fluorescently silent nGO/anti-miR-21/anti-miR-141 assembly, and the fluorescence intensities at FAM and Cy5 channels were measured at the end of the 2 h incubation period. Then, the fluorescence readings acquired with unknown samples were compared to the readings (520 and 670 nm) in the calibration plots obtained by standard miRNA solutions. We have observed a very strong agreement (around 90%) with the experimental results and the actual miRNA compositions, (Figure 3c). Both signals in FAM and Cy5 channels provide significant information about the content and the ratio of the oncomiRs in the cocktail. These results indicate that our approach enables simultaneous detection of both oncomiRs reliably with different expression levels.

We further studied the detection of both *miR*-21 and *miR*-141 from several human body fluids, since these two oncomiRs have been identified as circulating tumor biomarkers for prostate cancer diagnosis and disease staging. In order to demonstrate the detection of oncomiRs from body fluids, the total RNAs were extracted from human blood serum, saliva (both pellet and supernatant), and urine pellet. Later, separately, the RNA extraction was performed on each biological fluid after being enriched with exogenous *miR*-21 or *miR*-141. Finally, as a third set of experiments, the exogenous oncomiRs were added to the total RNAs extracted from body fluids. The resulting total RNA pool was composed of both

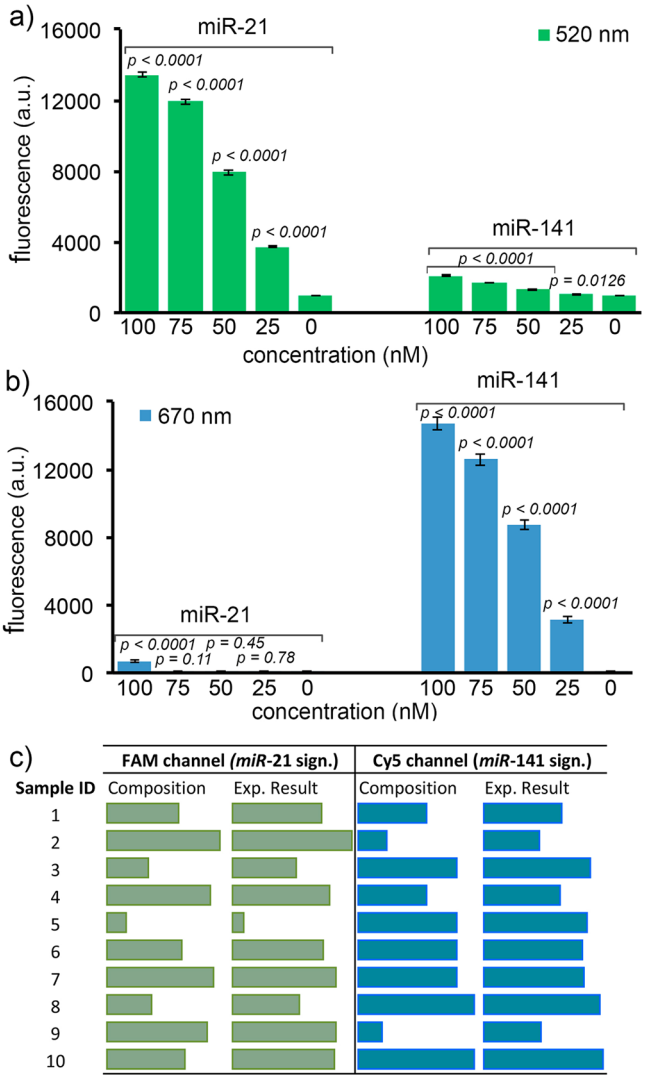

Figure 3. Fluorescence intensities spectra after 2 h of incubation with various concentrations of *miR*-21 and *miR*-141 at (a) 520 nm and (b) 670 nm. (c) Total fluorescence observed at 520 and 670 nm with 10 oncomiR cocktails with unknown concentrations and compositions. The experimental results were compared to calculated fluorescence recoveries based on the actual compositions. A very strong agreement (around 90%) between the experimental results and the actual miRNA compositions was observed. Experiments were performed in triplicate. Data are presented as mean ± s.d.

large and small RNAs, and exogenous oncomiRs. Eventually, five different samples were prepared from each single body fluid. For instance, [Serum RNA], [Serum RNA + *miR*-21]* before extraction, [Serum RNA + *miR*-21]** after extraction, [Serum RNA + *miR*-141]* before extraction, and [Serum RNA + *miR*-141]** after extraction were prepared from human blood serum. For the other biological samples, total RNAs were prepared with an analogous approach. Each sample was tested with the fluorescently silent nGO/anti-miR-21/anti-miR-141 complex. The fluorescence recoveries were obtained at 520 and 670 nm after 2 h of incubation.

First, the tests were performed on RNAs isolated from human serum. As seen in Figure 4a, serum RNA alone did not affect the emission at either wavelength and was comparable to the background signal (blank). On the other hand, [Serum RNA + miR-21]** showed the highest fluorescence signal

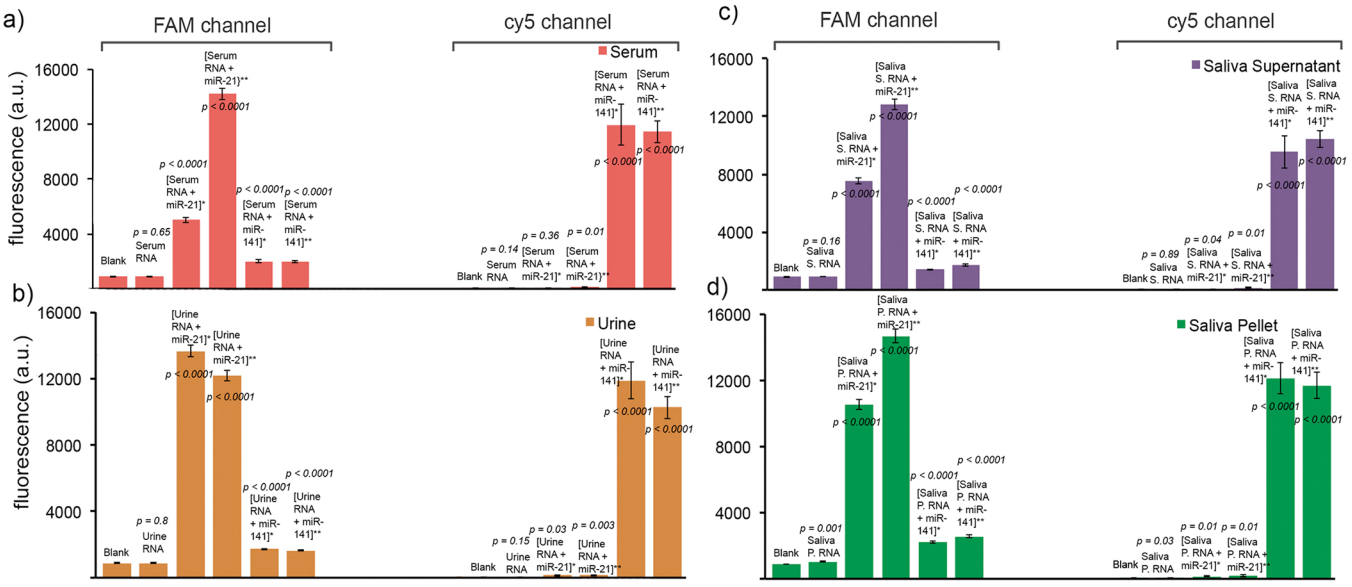

Figure 4. Fluorescence signals at FAM and Cy5 channels with human (a) serum, (b) urine, (c) saliva supernatant, and (d) saliva pellet provide information about the overexpressed *miR*-21 and *miR*-141 content. Experiments were performed in triplicate. Data are presented as mean ± s.d.

recovery at 520 nM. This was predicted since the total RNA content in this sample was the combination of extracted Serum RNA itself and exogenous *miR*-21. However, this sample had almost no effect on the emission at 670 nm, which was assigned as the signature of *miR*-141. Later, [Serum RNA + miR-21]* was tested with the nGO assembly, which caused a lesser, though significantly strong, signal at 520 nm. This was expected because the exogenous *miR*-21 was added into the serum before the RNA extraction was performed and a loss in the total RNA content is generally observed during the extraction process. Although a significantly strong signal at 520 nm was observed with this sample, the emission at 670 nm was at background values. Later, we tested to see whether *miR*-141 enriched biological fluids would have a similar effect at 670 nm emission. First [Serum RNA + miR-141]* and [Serum RNA + miR-141]** were tested with the nGO assembly. As seen, a remarkable recovery was observed with both samples at 670 nm; however, these two RNA pools had almost no effect on the fluorescence signals at 520 nm, which was assigned as the *miR*-21 signature. These results overall suggest that the total RNA extracted from human serum can enable us to detect two different circulating oncomiRs simultaneously, which could have significant implications in both detection of prostate cancer and identification of disease stages. Because the circulating oncomiRs are isolated in most of the body fluids we have performed analogous studies on saliva and urine samples.

For the saliva samples, both the saliva supernatant (Figure 4c) and saliva pellet (Figure 4d) showed significantly strong fluorescence signals with overexpressed target oncomiRs, comparable to serum data. For the detection of the overexpressed *miR*-21, [Saliva S. RNA + *miR*-21]** and [Saliva P. RNA + *miR*-21]** lead to a higher fluorescence recovery than [Saliva S. RNA + miR-21]* and [Saliva P. RNA + miR-21]*, respectively. However, these signals were significantly higher than [Saliva S. RNA] and [Saliva P. RNA], which were close to the background signal. As predicted, exogenous *miR*-141 enriched samples lead to an insignificant increase at 520 nm. In the Cy5 channel, however, both saliva samples with overexpressed *miR*-141 increased the fluorescence at 670 nm remarkably. On the other hand, samples with overexpressed *miR*-21 had almost no effect on the fluorescence signal at this wavelength, which was assigned as a signature of *miR*-141.

With the FAM parameters (Figure 4b), [Urine RNA + miR-21]* has the highest signal intensity as a result of a high-yield RNA extraction. [Urine RNA + miR-21]** caused slightly lower, yet still very strong, fluorescence recovery. As expected, samples with overexpressing *miR*-141 lead to an insignificant increase at 520 nm. For Cy5 readings (Figure 4b), again, [Urine RNA + miR-141]* and [Urine RNA + miR-141]** show a very strong fluorescence at 670 nm, whereas [Urine RNA] and urine samples with overexpressed *miR*-21 signals were almost identical to the background.

Although exogenous *miR*-21 or *miR*-141 signals are slightly lower or higher than each other in different samples, the critical inference here is that the fluorescence signal coming from the presence of overexpressed oncomiRs is significantly higher than the normal amount in the body fluids. This fundamental finding constitutes the essence of simultaneous detection of multiple circulating oncomiRs in body fluids in the case of aberrant expressions in specific cancer species. Detection of miRNAs is performed with different methods including PCR, blotting and microarray.[31] qRT-PCR enables the detection of multiple miRNAs simultaneously with a lower detection limit; however, it is a labor intensive and multistep process that requires expensive chemicals and machinery. Moreover due to the small size of miRNAs, the primers are short with low melting temperatures which influence the efficiency of the PCR.[31] Along with the above, the data analysis and interpretation of the results is complicated.[32] On the other hand, our approach is faster, easier and can be performed with a portable spectrofluorometer;[33] however, the sensitivity needs to be improved for a clinical application. Furthermore, our approach has the potential to be used as a cancer theranostic system for future applications of graphene oxide, which could enable in vivo oncomiR imaging and therapy.

In conclusion, miRNAs are very attractive diagnostic and therapeutic targets for the identification of the disease

dx.doi.org/10.1021/am504190a | ACS Appl. Mater. Interfaces 2014, 6, 14772−14778

stages—early, advanced, metastatic and nonmetastatic—of many cancer types from a variety of body fluids. Referred to as oncomiRs, they have been isolated from tumor tissues and most of the body fluids and are highly stable in the circulation. Here, we have designed a graphene oxide based nanoplatform, which enables simultaneous detection of two different circulating oncomiRs from human blood, saliva and urine. Each oncomiR, *miR*-21 or *miR*-141, is aberrantly expressed in the body fluids of prostate cancer patients and are the signatures of the disease stages. Nanographene oxide in this study serves as a highly stable and functional template in physiological buffer for the quick detection of both oncomiRs with different expressions. The extraordinary (ss)DNA adsorption capacity, and fast and ultraefficient fluorescence quenching capability of nGO lead us to engineer a fluorescently silent nanoplatform. However, because of the formation of DNA/miRNA hybrid structure in the presence of *miR*-21 or *miR*-141, enhanced fluorescence signals were observed at 520 and 670 nm, respectively. Overexpressed *miR*-21 resulted in a significant fluorescence increase only at 520 nm, whereas a fluorescence increase at 670 nm was observed with overexpressed *miR*-141 only. We have observed minor fluorescence increases with nontarget miRNAs because of replacement-induced desorption of probes from nGO surface. Since the copies of circulating miRNAs in patients' specimens are lower than the concentrations used in this study, and there are number of different miRNAs present in the body fluids, the detection limit and specificity has to be improved for a clinical scenario. On the basis of the current applications of nanographene in biomedicine and the role of circulating oncomiRs in cancer, the described biosensing design in this study has the potential to determine the early, advanced, metastatic, or nonmetastatic stages of prostate cancer with a non- or minimally invasive approach.

■ ASSOCIATED CONTENT

Ⓢ Supporting Information

Experimental details including materials and methods, and additional experimental results. This material is available free of charge via the Internet at http://pubs.acs.org/.

■ AUTHOR INFORMATION

Corresponding Author

*E-mail: myigit@albany.edu. Tel: (1) 518-442-3002.

Notes

The authors declare no competing financial interest.

■ ACKNOWLEDGMENTS

We thank Prof Igor Lednev for his assistance with the body fluid samples. We acknowledge the Ministry of National Education, Republic of Turkey, for providing financial support to Mustafa Salih Hizir with full scholarship during his doctoral studies.

■ REFERENCES

(1) Bartel, D. P. Micrornas: Genomics, Biogenesis, Mechanism, and Function. *Cell* **2004**, *116*, 281–297.

(2) Poy, M. N.; Eliasson, L.; Krutzfeldt, J. A Pancreatic Islet-Specific Microrna Regulates Insulin Secretion. *Nature* **2004**, *432*, 226–230.

(3) Robertson, N. M.; Yigit, M. V. The Role of Microrna in Resistance to Breast Cancer Therapy. *WIREs RNA* **2014**, DOI: 10.1002/wrna.1248.

(4) Esquela-Kerscher, A.; Slack, F. J. Oncomirs - Micrornas with a Role in Cancer. *Nat. Rev. Cancer* **2006**, *6*, 259–269.

(5) Reid, G.; Kirschner, M. B.; van Zandwijk, N. Circulating Micrornas: Association with Disease and Potential Use as Biomarkers. *Crit. Rev. Oncol. Hematol.* **2011**, *80*, 193–208.

(6) Garzon, R.; Calin, G. A.; Croce, C. M. Micrornas in Cancer. *Annu. Rev. Med.* **2009**, *60*, 167–179.

(7) Cortez, M. A.; Bueso-Ramos, C.; Ferdin, J.; Lopez-Berestein, G.; Sood, A. K.; Calin, G. A. Micrornas in Body Fluids–the Mix of Hormones and Biomarkers. *Nat. .Rev. Clin. Oncol.* **2011**, *8*, 467–477.

(8) Sita-Lumsden, A.; Dart, D. A.; Waxman, J.; Bevan, C. L. Circulating Micrornas as Potential New Biomarkers for Prostate Cancer. *Br. J. Cancer* **2013**, *108*, 1925–1930.

(9) Mitchell, P. S.; Parkin, R. K.; Kroh, E. M.; Fritz, B. R.; Wyman, S. K.; Pogosova-Agadjanyan, E. L.; Peterson, A.; Noteboom, J.; O'Briant, K. C.; Allen, A.; Lin, D. W.; Urban, N.; Drescher, C. W.; Knudsen, B. S.; Stirewalt, D. L.; Gentleman, R.; Vessella, R. L.; Nelson, P. S.; Martin, D. B.; Tewari, M. Circulating Micrornas as Stable Blood-Based Markers for Cancer Detection. *Proc. Natl. Acad. Sci. U.S.A.* **2008**, *105*, 10513–10518.

(10) Chen, X.; Ba, Y.; Ma, L.; Cai, X.; Yin, Y.; Wang, K.; Guo, J.; Zhang, Y.; Chen, J.; Guo, X.; Li, Q.; Li, X.; Wang, W.; Zhang, Y.; Wang, J.; Jiang, X.; Xiang, Y.; Xu, C.; Zheng, P.; Zhang, J.; Li, R.; Zhang, H.; Shang, X.; Gong, T.; Ning, G.; Wang, J.; Zen, K.; Zhang, J.; Zhang, C. Y. Characterization of Micrornas in Serum: A Novel Class of Biomarkers for Diagnosis of Cancer and Other Diseases. *Cell Res.* **2008**, *18*, 997–1006.

(11) Michel, S. C.; Keller, T. M.; Frohlich, J. M.; Fink, D.; Caduff, R.; Seifert, B.; Marincek, B.; Kubik-Huch, R. A. Preoperative Breast Cancer Staging: Mr Imaging of the Axilla with Ultrasmall Superparamagnetic Iron Oxide Enhancement. *Radiology* **2002**, *225*, 527–536.

(12) Yaman Agaoglu, F.; Kovancilar, M.; Dizdar, Y.; Darendeliler, E.; Holdenrieder, S.; Dalay, N.; Gezer, U. Investigation of Mir-21, Mir-141, and Mir-221 in Blood Circulation of Patients with Prostate Cancer. *Tumour Biol.* **2011**, *32*, 583–588.

(13) Schroder, F. H.; Roobol, M. J. Defining the Optimal Prostate-Specific Antigen Threshold for the Diagnosis of Prostate Cancer. *Curr. Opin. Urol.* **2009**, *19*, 227–231.

(14) Yildirim, A.; Acar, H.; Erkal, T. S.; Bayindir, M.; Guler, M. O. Template-Directed Synthesis of Silica Nanotubes for Explosive Detection. *ACS Appl. Mater. Interfaces* **2011**, *3*, 4159–4164.

(15) Hamner, K. L.; Maye, M. M. Thermal Aggregation Properties of Nanoparticles Modified with Temperature Sensitive Copolymers. *Langmuir* **2013**, *29*, 15217–15223.

(16) Wei, Q.; Nagi, R.; Sadeghi, K.; Feng, S.; Yan, E.; Ki, S. J.; Caire, R.; Tseng, D.; Ozcan, A. Detection and Spatial Mapping of Mercury Contamination in Water Samples Using a Smart-Phone. *ACS Nano* **2014**, *8*, 1121–1129.

(17) Huang, H.; Song, W.; Chen, G.; Reynard, J. M.; Ohulchanskyy, T. Y.; Prasad, P. N.; Bright, F. V.; Lovell, J. F. Hydrogels: Pd-Porphyrin-Cross-Linked Implantable Hydrogels with Oxygen-Responsive Phosphorescence. *Adv. Healthcare Mater.* **2014**, *3*, 891–896.

(18) Liu, T.; Wang, C.; Gu, X.; Gong, H.; Cheng, L.; Shi, X.; Feng, L.; Sun, B.; Liu, Z. Drug Delivery with Pegylated Mos2 Nano-Sheets for Combined Photothermal and Chemotherapy of Cancer. *Adv. Mater.* **2014**, *26*, 3433–3440.

(19) Huang, P.-J.; Liu, J. Separation of Short Single- and Double-Stranded DNA Based on Their Adsorption Kinetics Difference on Graphene Oxide. *Nanomaterials* **2013**, *3*, 221–228.

(20) Huang, P.-J. J.; Kempaiah, R.; Liu, J. Synergistic Ph Effect for Reversible Shuttling Aptamer-Based Biosensors between Graphene Oxide and Target Molecules. *J. Mater. Chem.* **2011**, *21*, 8991–8993.

(21) Yang, K.; Feng, L.; Shi, X.; Liu, Z. Nano-Graphene in Biomedicine: Theranostic Applications. *Chem. Soc. Rev.* **2013**, *42*, 530–547.

(22) Lu, Z.; Zhang, L.; Deng, Y.; Li, S.; He, N. Graphene Oxide for Rapid Microrna Detection. *Nanoscale* **2012**, *4*, 5840–5842.

(23) Balcioglu, M.; Rana, M.; Yigit, M. V. Doxorubicin Loading on Graphene Oxide, Iron Oxide and Gold Nanoparticle Hybrid. *J. Mater. Chem. B* **2013**, *1*, 6187−6193.
(24) Liu, J. Adsorption of DNA onto Gold Nanoparticles and Graphene Oxide: Surface Science and Applications. *Phys. Chem. Chem. Phys.* **2012**, *14*, 10485−10496.
(25) Rana, M.; Balcioglu, M.; Robertson, N.; Yigit, M. V. Nano-Graphene Oxide as a Novel Platform for Monitoring the Effect of Lna Modification on Nucleic Acid Interactions. *Analyst* **2014**, *139*, 714−720.
(26) Cui, L.; Lin, X.; Lin, N.; Song, Y.; Zhu, Z.; Chen, X.; Yang, C. J. Graphene Oxide-Protected DNA Probes for Multiplex Microrna Analysis in Complex Biological Samples Based on a Cyclic Enzymatic Amplification Method. *Chem. Commun.* **2012**, *48*, 194−196.
(27) Bai, Y.; Feng, F.; Zhao, L.; Chen, Z.; Wang, H.; Duan, Y. A Turn-on Fluorescent Aptasensor for Adenosine Detection Based on Split Aptamers and Graphene Oxide. *Analyst* **2014**, *139*, 1843−1846.
(28) Chen, K.; Lu, G.; Chang, J.; Mao, S.; Yu, K.; Cui, S.; Chen, J. Hg(Ii) Ion Detection Using Thermally Reduced Graphene Oxide Decorated with Functionalized Gold Nanoparticles. *Anal. Chem.* **2012**, *84*, 4057−4062.
(29) Jung, Y. K.; Lee, T.; Shin, E.; Kim, B. S. Highly Tunable Aptasensing Microarrays with Graphene Oxide Multilayers. *Sci. Rep.* **2013**, DOI: 10.1038/srep03367.
(30) Wu, M.; Kempaiah, R.; Huang, P. J.; Maheshwari, V.; Liu, J. Adsorption and Desorption of DNA on Graphene Oxide Studied by Fluorescently Labeled Oligonucleotides. *Langmuir* **2011**, *27*, 2731−2738.
(31) Cissell, K. A.; Shrestha, S.; Deo, S. K. Microrna Detection: Challenges for the Analytical Chemist. *Anal. Chem.* **2007**, *79*, 4754−4761.
(32) Kroh, E. M.; Parkin, R. K.; Mitchell, P. S.; Tewari, M. Analysis of Circulating Microrna Biomarkers in Plasma and Serum Using Quantitative Reverse Transcription-Pcr (Qrt-Pcr). *Methods* **2010**, *50*, 298−301.
(33) Coskun, A. F.; Nagi, R.; Sadeghi, K.; Phillips, S.; Ozcan, A. Albumin Testing in Urine Using a Smart-Phone. *Lab Chip* **2013**, *13*, 4231−4238.